Dynamics of Electron Flux in the Slot Region and Geomagnetic Activity

Lidia Nikitina[1] and Larisa Trichtchenko[1]

[1]Natural Resources Canada

November 24, 2022

Abstract

The slot region between the radiation belts in the magnetosphere is considered to be stable and safe for satellite missions, but strong disturbances during space weather events can cause an enhancement of the electron radiation environment in this area. This paper provides an analysis of the dynamics of electron flux in 1998-2007 with specific attention to slot filling events and preceded geomagnetic activity. Flux of energetic electrons, with energies E>0.63 MeV, E>1.5 MeV, and E>3 MeV, was obtained from detectors on board the HEO-3 satellite in highly elliptical orbit. To evaluate geomagnetic conditions, associated with enhancement of electron flux, all the 'slot filling events' were studied together with geomagnetic activity provided by Dst and Kp global indices as well as with thehourly range indices of geomagnetic variations at mid-latitude. These geomagnetic indices were used for assessment of a threshold and frequency of occurrence of slot filling events. Regression analysis has been used to find a relationship between the maximum filling of the slot region due to space weather event and preceding geomagnetic activity level. Influence of the cumulative time of periods of enhanced geomagnetic activity to the variation of the electron flux in the slot region has been analysed. Suitability of different indices of geomagnetic activity for estimation of rate of occurrence of slot filling events and for assessment of electron flux in the slot region is discussed.

Dynamics of Electron Flux in the Slot Region and Geomagnetic Activity

L. Nikitina[1], L.Trichtchenko[1]

[1]Geomagnetic Laboratory, Natural Resoures Canada, Ottawa, Ontario, Canada.

Corresponding author: Lidia Nikitina (lidia.nikitina@canada.ca)

Key Points:

- Electron flux in the slot region was analysed based on highly elliptical orbit satellite data for 1998 - 2007
- Frequency and intensity of slot filling events were determined for different levels of geomagnetic activity
- Geomagnetic indices better suited for assessment of electron flux in the slot region were identified

Abstract

The slot region between the radiation belts in the magnetosphere is considered to be stable and safe for satellite missions, but strong disturbances during space weather events can cause an enhancement of the electron radiation environment in this area. This paper provides an analysis of the dynamics of electron flux in 1998-2007 with specific attention to slot filling events and preceded geomagnetic activity. Flux of energetic electrons, with energies E>0.63 MeV, E>1.5 MeV, and E>3 MeV, was obtained from detectors on board the HEO-3 satellite in highly elliptical orbit. To evaluate geomagnetic conditions, associated with enhancement of electron flux, all the 'slot filling events' were studied together with geomagnetic activity provided by Dst and Kp global indices as well as with thehourly range indices of geomagnetic variations at mid-latitude. These geomagnetic indices were used for assessment of a threshold and frequency of occurrence of slot filling events. Regression analysis has been used to find a relationship between the maximum filling of the slot region due to space weather event and preceding geomagnetic activity level. Influence of the cumulative time of periods of enhanced geomagnetic activity to the variation of the electron flux in the slot region has been analysed. Suitability of different indices of geomagnetic activity for estimation of rate of occurrence of slot filling events and for assessment of electron flux in the slot region is discussed.

1. Introduction

Interest in the radiation environment of the slot region which separates the two electron radiation belts is motivated by the increasing number of scientific and service satellites with orbits that take them through this region, for example, Galileo constellation. Traditionally, the radiation environment in the slot region has been considered to be stable with low level of radiation (Lyons & Thorne, 1973), which is benign conditions for satellites; but data obtained during recent decades demonstrate large variability of the electron flux, especially after strong space weather events (see, e.g. Baker et al., 2004; Kavanagh et al., 2018; Reeves et al., 2016; Turner et al., 2015; Zhao et al., 2016; Zhao & Li, 2013a,b). New data motivated studies and development of models of radiation environment in the slot region (Sandberg et al., 2014; Sicard-Piet et al., 2014).

Variability of electron flux in the slot region is defined by two time-scales. Filling of the slot by relativistic electrons after a geomagnetic storm takes several days (usually 2-3 days for E > 1 MeV, see, e.g. Baker et al., 1994). During these days the electron flux is usually increased by 2-3 orders of magnitude compared to pre-storm levels. The subsequent gradual decrease takes from tens to hundreds of days depending on electrons energy and L-value (Baker et al., 1994; Meredith et al., 2007; Reeves et al., 2016; Ripoll et al., 2015). This long decay of electrons in the slot makes every slot filling event significant for the average radiation conditions in this region.

Although it is commonly accepted that the dynamics of electron flux in the radiation belts is defined by a balance between processes of inward radial diffusion, and acceleration and loss through resonant interaction between electrons and magnetospheric waves, the exact space weather conditions and mechanisms of the slot filling are still under discussion (see review by Baker et al., 2018 and references therein).

Relation between large geomagnetic variations and filling of the slot region has been discussed in numerous studies, e.g. Thorne et al. (2007), Tverskaya (2011). Importance of storm and substorm geomagnetic activity for the formation of the slot region was pointed out in Tsurutani et al. (2018) as well as in Falkowski et al. (2017), Meredith et al. (2007), Lazutin and Kozelova (2011), and Nagai et al. (2006). It is known that the penetration distance of electrons into the slot region has a correlation with the daily minimum value of Dst (Tverskaya, 2011). On the other side, it is known that not all strong space weather events are followed by enhancement of electron flux in the slot region. The analysis of slot filling events in 1995-2003 for 2-6 MeV electrons in Zheng et al. (2006) and Zhao and Li (2013a) found that of 55 magnetic storms with abs(Dst) exceeding 130 nT there were only 22 that were followed by injection of electrons into the middle part of the slot region (L = 2.5).

The aim of the present study is to analyse slot filling in relation to the level of geomagnetic activity as given by Dst and other indices. For this purposes, all slot filling events (hereinafter referred to as SF events), derived with the use of data from HEO-3 mission in 1998-2007 years (obtained from the Aerospace Corporation at http://virbo.org/HEO) were analysed together with the corresponding geomagnetic activity. This data set covers 10 years and, therefore, provides an opportunity to analyse variability of the slot electron environment for almost an entire solar cycle.

For analysis of geomagnetic conditions preceding each SF event, Dst index, Kp index and the hourly range indices of geomagnetic activity were utilised.

To detect the SF events, at first their location has been defined as the region inside the slot where flux is statistically independent from flux in the inner and outer electron belts. Then SF events were identified and studied together with the corresponding geomagnetic activity to define the thresholds for SF events to occur, and their rate of occurrence.

To determine a quantitative relationship between intensification of electron flux in the slot and preceding geomagnetic disturbances, a regression analysis was performed between geomagnetic activity and maximum electron flux per event. Long-term variation of the electron flux in the slot region was analyzed in relation to the cumulative time of periods of enhanced geomagnetic activity.

An analysis has also been made of the suitability of different indices of geomagnetic activity for estimation of the rate of occurrence of SF events and for assessment of electron flux in the slot.

The paper is structured as follows. Section 2 describes the electron flux data used for the analysis. Section 3 provides a statistical description of electron flux in the slot region and justification for the selection of the range of L-shells which is used for analysis of SF events. Section 4 provides an example of the dynamics of electrons and associated geomagnetic activity during a strong space weather event (July 15th -16th, 2000). Sections 5 presents general criteria used for identification of SF events and the list of events in 1998-2007 based on HEO-3 data. In sections 6-8, thresholds and rate of occurrence of SF events are determined for each of these global geomagnetic indices abs(Dst) and Kp, as well as for local hourly range indices at several geomagnetic observatories with their corresponding L-values close to the L-range for the slot. Section 9 provides results of the regression analysis of the relationship between enhanced values of the electron flux in the slot region and preceding geomagnetic activity. Relation between the cumulative time of enhanced geomagnetic activity and variability of electron fluxes is discussed in Section 10. Results are summarised in Section 11.

2. Electron flux data used for the analysis

The energetic electron data which have been analysed here were recorded in a highly elliptical orbit by the HEO-3 mission in 1998-2007. Data from HEO-3 detectors in the E > 0.63 MeV, E > 1.5 MeV, and E > 3 MeV energy bands are available as 15-second averages and binned by the Roederer invariant magnetic coordinate L (sometimes cited as L*) (Roederer, 1970; Roederer and Lejosne, 2018).

Orbital period of the HEO satellite is close to 12 hours, orbit's apogee ~ 40,000 km and perigee ~ 1000 km with orbit inclination of about 63°. This orbit covers L values in the range 1.8-8.0, extending from the outer edge of the inner electron belt, through the slot region and the outer electron belt. There are two orbits per day; for consistency and to minimize the discrepancies in fluxes which might be caused by the differences between even and odd orbits, the data from the outbound segment of the even orbit (i.e. one segment per day) were used in the analysis.

The electron flux in the energy channel E > 3 MeV for the total duration under study, i.e. 1998-2007, obtained from HEO-3 is presented in Figure 1. As can be seen, the segment of the orbit used in this study provides electron flux for the outer edge of the inner electron belt close to L=1.8-2.0, for the slot region (with minimum value of the electron flux) at L=2.0-3.0 and for the most of the outer radiation belt with L in the range L=3.0 - 6.5. Green color on this plot corresponds to flux values less than 50 cm^{-2} s^{-1} sr^{-1}. The inner boundary of the "green zone" is almost constant, at L=2.0-2.2, and the outer boundary of the "green zone" varies in the range from L=2.5 to L=3.5.

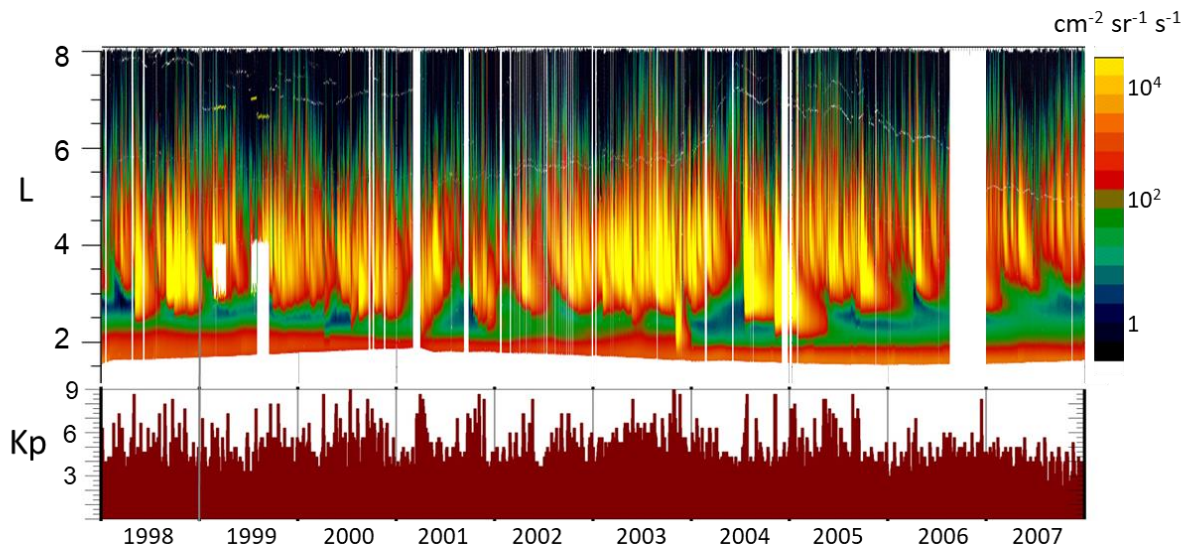

Figure 1. Electron flux E > 3 MeV measured on HEO orbit (upper panel), Kp index (bottom panel), 1998-2007.

Usual position of the slot region is assumed to be located roughly between L ~ 2 and L ~ 3, depending on energy (Baker et al., 2018). However, Figure 1 shows that this region exhibits large variability of the electron flux. Thus, in the period 1998-2007 this region has been filled several times by energetic electrons with increases of the electron flux by several orders of magnitude.

These times are usually related to increases of geomagnetic activity (see Kp index plot, Figure 1, bottom panel).

3. Statistical variability of electron flux along the HEO-3 orbit

The whole period of 1998-2007 years has been used for derivation of the general statistical parameters for each electron energy band in the region L=1.5-5.0. Figure 2 provides the basic statistics for the electron flux. Statistics include mean (dash green curve), median (brown curve), 95 percentile (red), and 99 percentile (blue). The large variability of the flux between the external boundary of the inner radiation belt at L~2.0 and the internal boundary of the outer radiation belt with L~3.0 (shaded gray area) is clearly seen as 2.5-3 orders of magnitude difference between median (50%, brown) and 99% (blue) curves.

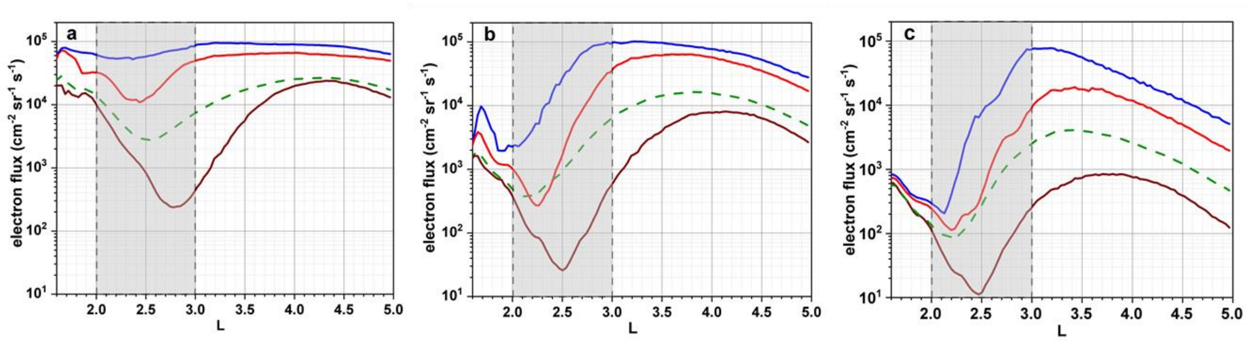

Figure 2. Percentiles of electron fluxes in the electron belts and the slot in 1998-2007, a) E > 0.63 MeV, b) E > 1.5 MeV, c) E > 3 MeV. Blue line – 99th percentile curve, red – 95th percentile curve, green – mean curve, brown – median curve.

The median electron flux curve (50% percentile) can be considered as a quiet time curve. The centre of the slot at the quiet (median) curve is located close to L=2.75 for electrons with energy > 0.63 MeV, and close to L=2.5 for E > 1.5 MeV and E > 3 MeV. The mean and larger percentile curves (95^{th} and 99^{th}) have the centre (i.e. location of the minimal values of electron flux) shifted to L below 2.5 for E >0.63 MeV and to L below 2.2 for E >1.5 MeV and E > 3 MeV with respect to the corresponding median curve.

To clearly define an area in the slot region which can be used for study of SF events, the influence of the inner and outer electron belts on the flux inside the area L=2.0-3.8 has been evaluated for two periods of time, for an active year 1998 with several strong magnetic storms, and for a quiet period, corresponding to the first half of year 2006. This has been done by the estimation of correlations of the flux for L-bins inside 2.2 < L < 3.8, ΔL=0.2, with each of: the electron flux in the inner electron belt (L=1.8-2.0) and in the outer electron belt (L=3.8-4.0). The results obtained are shown in Figure 3, where the red curve represents correlation with the inner belt and the green curve represents correlation with the outer belt. It can be concluded that during the active year 1998 (Figure 3a,b,c), the effect from the inner electron belt (green curves) is significant up to L values 2.2, with correlation coefficients higher than 0.45 in all three energy bands. Impact from the outer electron belts (red curves) is significant for L > 2.8 in E > 0.63 MeV and E > 1.5 MeV energy bands with correlation coefficients higher than 0.55, and for L > 2.9 in E > 3 MeV with correlation coefficients higher than 0.5.

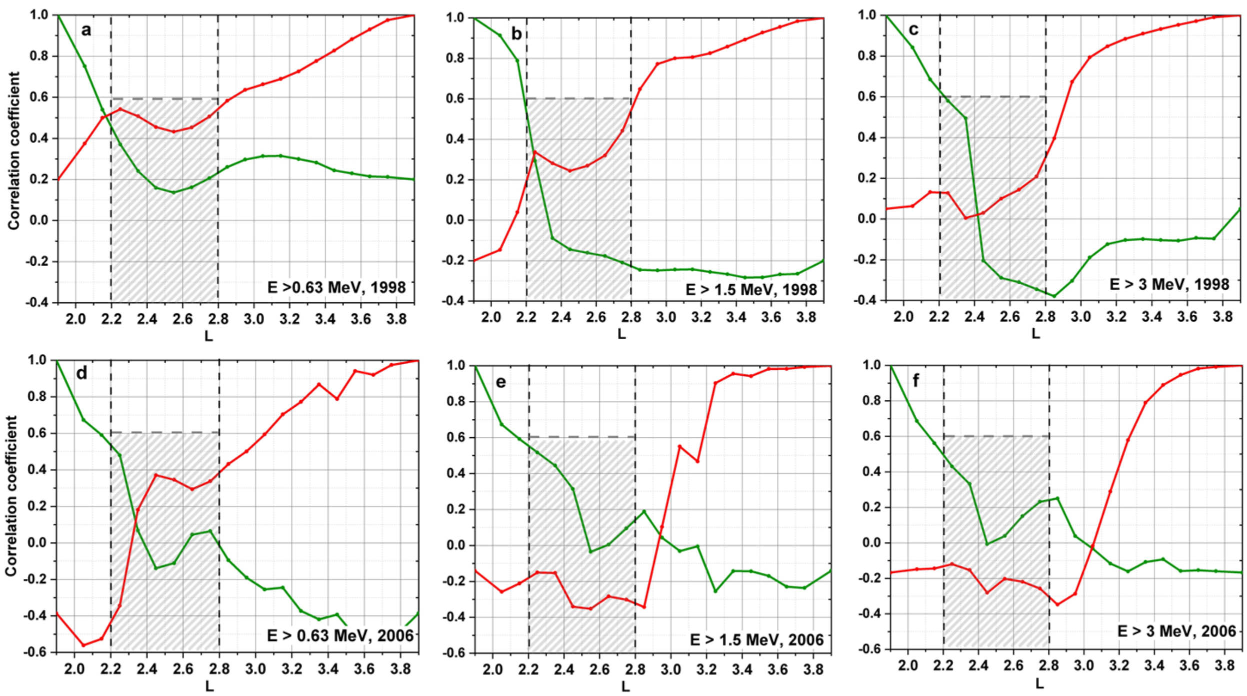

Figure 3. Correlation of electron flux in the slot and electron flux in the inner electron belt (green line) and the outer electron belt (red line). Left panels (a,d) for E >0.63 MeV, central panels (b, e) for E > 1.5 MeV, right panels (c, f) for E > 3 MeV. Upper panel (a,b,c) for an active period (year 1998); bottom panels (d,e,f) for a quiet period (first half of year 2006). Shadow area demonstrates that all the correlation curves are below 0.6 inside L=2.2-2.8.

For the quiet interval in 2006 (panels d,e,f on Figure 3), correlation coefficients with the inner electron belt L are higher than 0.55 for L < 2.2 in all three energy channels, similar to an active year, but the influence of the outer electron belt does not propagate so deep, the correlation coefficient exceeds 0.5 for L > 2.9 in energy band E > 0.63 MeV and for L > 3.1-3.2 in energy bands E > 1.5 MeV and E > 3 MeV.

Thus, further analysis has been made for the interval L=2.2-2.8, where influence of both inner and outer electron belts are not statistically significant (which is demonstrated by the shadow area on Figure 4, a-d, with correlation below 0.6), and where the minima of median and mean are located (see Figure 2), making this interval representative for the dynamics of electron flux in the slot region.

Statistical distribution of the electron flux in the slot region is presented in Figure 4 where histograms are plotted for the daily values (averaged in the interval L=2.2-2.8) during an active (2003) and a quiet (2007) years for E >1.5 MeV. Histogram for the daily values of electron flux in the slot in 2003 have a long-tail distribution with the largest value achieving $7.7 \cdot 10^4$ $cm^{-2}s^{-1}$ sr^{-1} (Figure 4a) while the daily values of electron flux during quiet year 2007 (Figure 4b) are inside the range 25-95 $cm^{-2}s^{1}sr^{-1}$ (this range is less than one bin on Figure 4a). All the statistical values for these two years are provided in Table 1 and demonstrate several orders of magnitude difference between quiet and active years in all three energy channels.

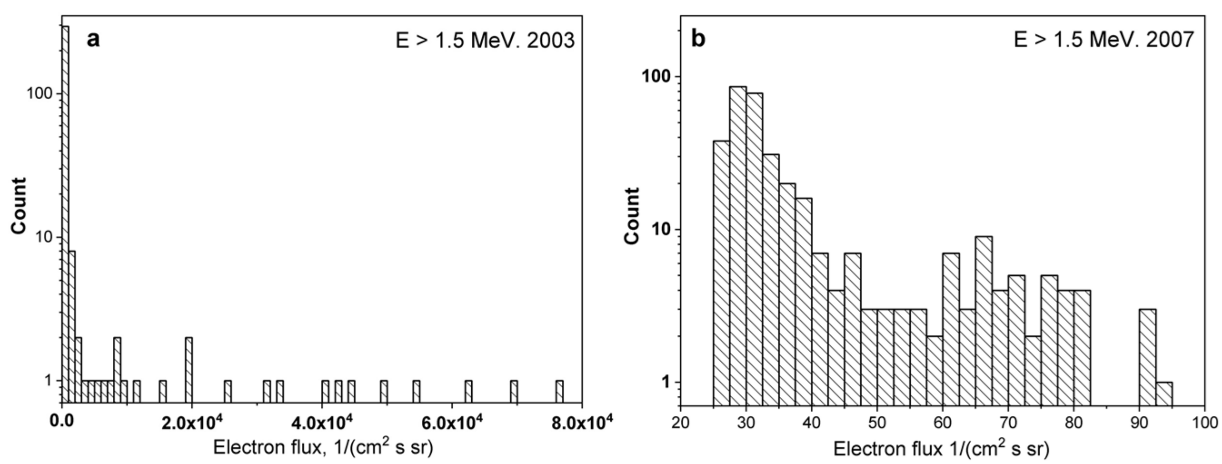

Figure 4. Histograms of the daily mean value of the electron flux E > 1.5 MeV in the slot region, L=2.2-2.8, for an active year (2003, left panel, bin size 100 $cm^{-2}s^{-1}$ sr^{-1}) and for a quiet year (2007, right panel, bin size 5 $cm^{-2}s^{-1}$ sr^{-1})

Table 1.

Statistics of the Electron Flux in the Range L=2.2-2.8 for an Active Year (2003) and a Quiet Year (2007)

	E > 0.63 MeV,	E > 1.5 MeV	E > 3 MeV,

	($cm^{-2}s^{-1}$ sr^{-1})		($cm^{-2}s^{-1}$ sr^{-1})		($cm^{-2}s^{-1}$ sr^{-1})	
Year	2003	2007	2003	2007	2003	2007
Median	1550	1025	167	31	78	13
Mean	5110	1135	2200	38	550	20
St. dev	11700	360	9300	15	2060	17
Max	74400	2800	76600	94	14945	80

4. Dynamics of slot electron flux and geomagnetic activity

Typical scenario of filling of the slot region can be illustrated by a strong space weather event on July, 15-16th 2000. Figure 5 shows the penetration of electrons E > 3 MeV into the slot region during this event. The left panel represents the overall dynamics of electrons from June to August 2000 which clearly demonstrates the injection of electrons into the slot region in the middle of July. The right panel of Figure 5 shows the daily variations of electrons with L-value for the days, July 14-22, 2000. Green curve for July 14th corresponds to quiet conditions preceding this SF event with peak values at L ~ 1.9 and L ~ 3.3 related to pre-event location of the inner and outer electron belts. Strong geomagnetic variations on July 15th were followed by a sharp decrease of the electron flux across all L-values (yellow curve, July 15th) and subsequent growth of the flux at the new location around L ~ 2.7-2.8 (yellow curve on July 17th). Maximum filling of the slot region was achieved on July 19th (red curve), which was followed by attenuation of the flux inside the slot region and recovering of the outer electron belt, shown by the curve for July 22nd (brown) which has two local maxima, one close to L~2.9 and another at L~3.8.

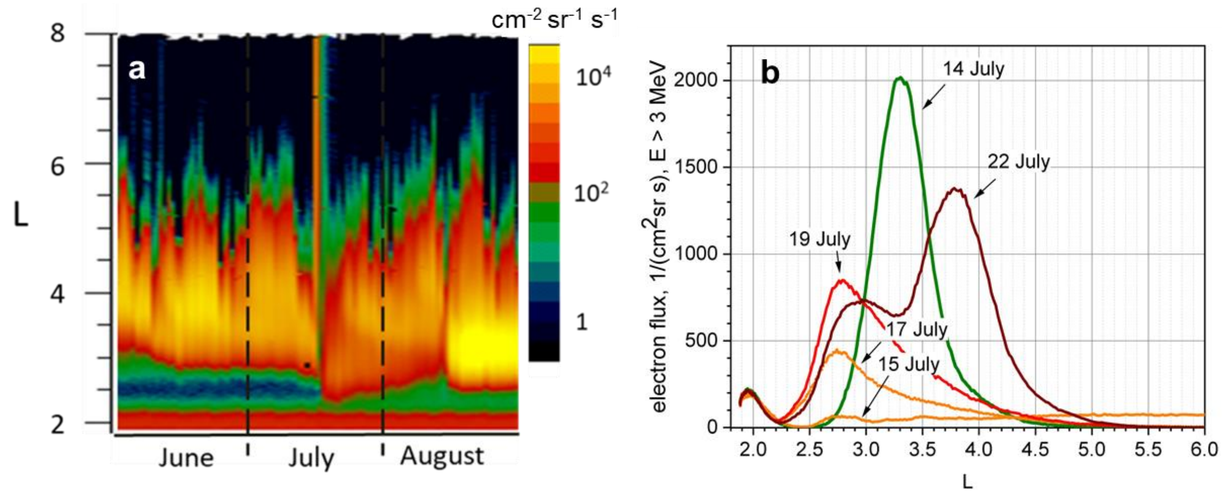

Figure 5. Dynamics of the electron flux preceding, during, and after space weather event on July,15-16, 2000, E > 3 MeV; a) electron flux during three months, June - August 2000; b) daily curves of the electron flux for 14-22 July, 2000.

Dynamics of daily mean electron flux in the interval L=2.2-2.8 for this event together with variations of several geomagnetic indices are presented on Figure 6, covering the period July 8 to August 7, 2000 (days of the year 190-220). On Figure 6a, the red curve provides electron flux for E > 0.63 MeV, green curve for E > 1.5 MeV and blue curve for E > 3 MeV. Daily values of geomagnetic indices are plotted on panels below, maximum daily value of abs(Dst) on Figure 6b and daily maximum of Kp index on 6c.

Figures 6b-6c demonstrate that, during the space weather event, the largest disturbances in the geomagnetic field were recorded on days 197-198 (15-16 July). Kp index reached a value of 9 and Dst index dropped to –289 nT on day 197 and to –301 nT on day 198. Figure 6a shows that filling of the slot region (sharp increase of the electron flux in L=2.2-2.8) starts on day 198 (16th of July), and the flux achieves its maximum on days 200-201 (18 – 19 July), four days after the magnetic storm starts. For the event considered the electron flux increased by 55 times for E > 0.63 MeV, by 136 times for E > 1.5 MeV and by 9 times for E > 3 MeV. After the peak, the electron flux declines for the next 20 days but did not return to pre-event conditions because of the new event on 12th of August 2000 (seen in the left panel of Figure 5).

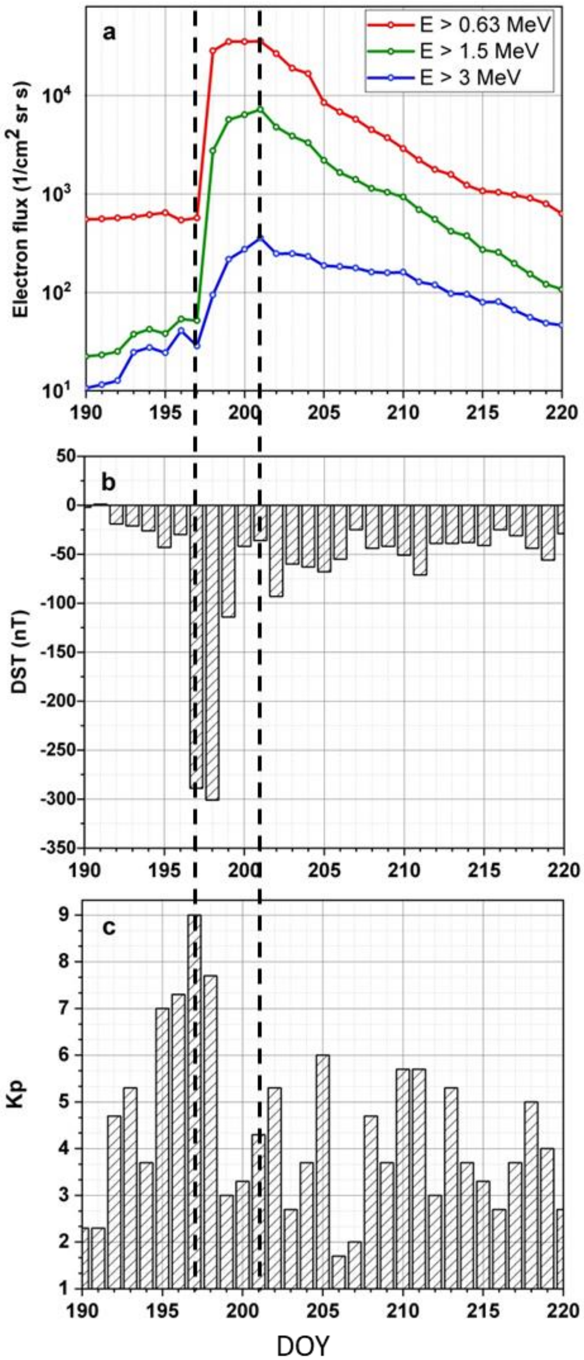

Figure 6. Electron flux in the slot and geomagnetic variations during 18 July – 7 August, 2000 (days of the year: 190-220); a) daily mean electron flux in the region L=2.2-2.8 in E > 0.63 MeV (red), E >1.5 MeV (green), E > 3 MeV (blue); b) daily maximum value of abs(Dst); c) daily maximum value of Kp.

5. List of SF events and related geomagnetic activity

For the complete analysis of SF events, all the cases when the daily mean value of the electron flux in the region L= 2.2-2.8 increased at least twice comparing to pre-storm conditions were analysed together with preceding geomagnetic disturbances. The following criteria were applied: pre-storm electron flux is defined as the maximum during 3 days preceding the magnetic storm, and post-storm flux is defined as a maximum during 7 days after the storm. This approach is similar to the approach suggested by Reeves et al. (2003) for analysis of the response of the outer electron belt to geomagnetic storms. If the post-storm electron flux in the slot region achieved values at least twice as large as pre-storm flux, this event has been considered a 'slot filling event'. A short dropout of the electron flux in the slot which is usually observed at the beginning of the magnetic storm (see, e.g. Onsager et al., 2002) was ignored and the peak value of the electron flux which is achieved several days after (usually 3-4 days) was considered.

Table 2 presents all SF events (35), identified for the years 1998-2007 for each energy channel, where '1' denotes the slot event, '0' corresponds to 'no event'. The day with the maximum value of abs(Dst) per event is defined as the day of the event in the table. Kp index in the table corresponds to its maximum value per event, even if it is related to day other than the abs(Dst) maximum. When two events happen very close each other, for example, two magnetic storms which occurred on 29 and 30 October 2003, the flux before the first event is compared with the flux after the second event. In the table the day with the largest abs(Dst) among both is provided. Overall, in 1998-2007, the SF events were identified 34 times in energy channel E > 0.63 MeV, 25 times in E > 1.5 MeV, and 19 times in E > 3 MeV. Only 18 of these events were recorded simultaneously in all three energy channels.

It was concluded in many studies that SF events are more often identified in lower energies (see, e.g. Zhao and Li, 2013b). Thus, analysis of SF events in year 2013 (Reeves et al., 2016), notes several events for electrons with energy ≤ 459 keV, while for the same period, there were no SF events for electrons E > 1.5 MeV. Table 2 demonstrates as well that almost all SF events which are identified in higher energy channels are also seen in lower energy channels, with the exception of event # 19 (May 23, 2002). During this event, the electron flux for E > 3 MeV doubled compared to the day before the event, but the increasing of electrons in the two other channels was not sufficient to pass our conditions (about 7% increase for E > 0.63 MeV and about 40% in for E

> 1.5 MeV comparing to pre-event conditions), thus it is denoted as ‘no event’ in Table 2. Two of events in Table 2 (denoted as *) were followed by a decrease of the electron flux for E > 3 MeV in the slot region. These events are discussed in the next section.

Table 2. *List of slot filling events. ‘1’ denotes the slot filling event; ‘0’ – no event*

	Year	Day of the year	Date	Kp	Abs(Dst), nT	E > 0.63 MeV	E > 1.5 MeV	E > 3 MeV
1	1998	124	May 4	9-	205	1	1	1
2	1998	218	Aug 6	7+	138	1	0	0
3	1998	239	Aug 27	8	155	1	1	0
4	1998	268	Sep 25	8+	207	1	1	1
5	1998	312	Nov 8	8-	149	1	1	0
6	1999	295	Oct 22	8	237	1	1	0
7	2000	97-98	Apr 6-7	9-	288	1	1	1
8	2000	198	July 16	9	301	1	1	1
9	2000	225	Aug 12	8-	235	1	1	1
10	2000	279	Oct 5	8-	182	1	1	1
11	2000	311	Nov 6	7	159	1	1	1
12	2001	90	Mar 31	9-	387	1	1	1
13	2001	101	Apr 11	8+	271	1	0	0
14	2001	276	Oct 3	7	166	1	1	1
15	2001	294	Oct 21	8-	187	1	1	1
16	2001	310	Nov 6	9-	292	1	1	0
17	2001	328	Nov 24	8+	221	1	1	1

18	2002	110	Apr 20	7+	149	1	1	0
19	2002	143	May 23	8+	109	0	0	1
20	2002	251	Sep 8	7+	181	1	0	0
21	2002	274	Oct 1	7+	176	1	1	0
22	2003	149	May 29	8+	144	1	1	1
23	2003	169	Jun 18	7-	141	1	0	0
24	2003	230	Aug 18	7+	148	1	1	1
25	2003	303	Oct 30	9	383	1	1	1
26	2003	324	Nov 20	9-	422	1	0	0 (*)
27	2004	22	Jan 22	7	130	1	0	0
28	2004	209	Jul 27	9-	170	1	1	1
29	2004	313	Nov 8	9-	374	1	1	1
30	2005	22	Jan 22	8	97	1	0	0
31	2005	128	May 8	8+	110	1	0	0
32	2005	135	May 15	8+	247	1	1	0 (*)
33	2005	236	Aug 24	9-	184	1	1	1
34	2005	254	Sep 11	8-	139	1	1	1
35	2006	104	Apr 14	7	98	1	0	0

Note. (*) denotes decrease of the electron flux in the slot after the event. [1]Date of the storm corresponds to the maximum value of abs(Dst) during the event.

6. SF events and Dst index

Correspondence between variations of the electron flux in the outer radiation belt and the Dst index has been identified in a number of investigations, with the most popular formula for evaluation of the position of the outer belt maximum (Tverskaya, 2011). Thus, as SF events are associated with strong space weather events, with the inward movement of the outer radiation belt and high relativistic electrons at the outer edge of the slot region which are related to Dst index (see, e.g. Baker, 2018), the statistical analysis of both of them, i.e. space weather events as characterised by Dst, and SF events as characterised by flux of electrons has been accomplished as follows.

From Table 2, it can be inferred that none of the SF events happened while the absolute Dst value was less than 95 nT. The total number of space weather events in 1998-2007 with the abs(Dst) ≥ 95 nT was 71. Approximately half of them (35) were followed by SF events. Rate of occurrence for SF events associated with different values of abs(Dst) is presented in Figure 7.

Figure 7a provides the number of occurrence of SF events. The grey columns correspond to number of all space weather events when the maximum value of abs(Dst) for event was in a given bin, bin size is 20 nT. The green, orange and red columns represent number of SF events determined in a given bin for 0.63 MeV, 1.5 MeV, and 3 MeV correspondingly. Figure 7b provides the relative rate of occurrence of SF events and demonstrate overall increase of the rate of occurrence with increase of abs(Dst).

Only a few magnetic storms with 95nT < abs(Dst) < 140 nT were followed by SF events, i.e. six for E > 0.63 MeV, one for E > 1.5 MeV and two for E > 3 MeV. Among the 12 space weather events with abs(Dst) between 140 nT and 180 nT, filling of the slot was detected 10 times for electrons E > 0.63 MeV, 9 times for E > 1.5 MeV and 4 times for E > 3 MeV. Space weather events with abs(Dst) > 180 nT significantly affect the slot region. All of these 18 events caused enhancement of the electron flux in the slot in E > 0.63 MeV (100% rate of occurrence), 15 of them caused SF events in electrons E >1.5 MeV (83%) and 12 for electrons E > 3 MeV (67 %).

Two of these magnetic storms were followed by a decrease of the previously enhanced electron flux in the slot region for E > 3 MeV (denoted by ‘star’ in Table 2). The first case was recorded after the magnetic storm on November 20th 2003 (# 26, Table 1), with Dst = -422 nT, when E > 3 MeV electron flux sharply decreased by more than order of magnitude. This magnetic storm happened very soon after the Halloween storm (October 2003 #25, Table 2). The electron flux in the slot region remained very high after the Halloween storm, and, most likely, the dynamics of electrons in the slot region and in the outer radiation belt was under the influence of recovery processes after the previous magnetic storm. The exceptional dynamics of electrons on November, 20th, 2003 was also examined by Tverskaya et al., 2011, based on data from CORONAS-F satellite at LEO. She pointed out that the November 20, 2003 magnetic storm caused injection of electrons with energies 0.6-1.5 MeV into the slot, but fluxes of electrons with higher energy decreased by more than two orders of magnitude.

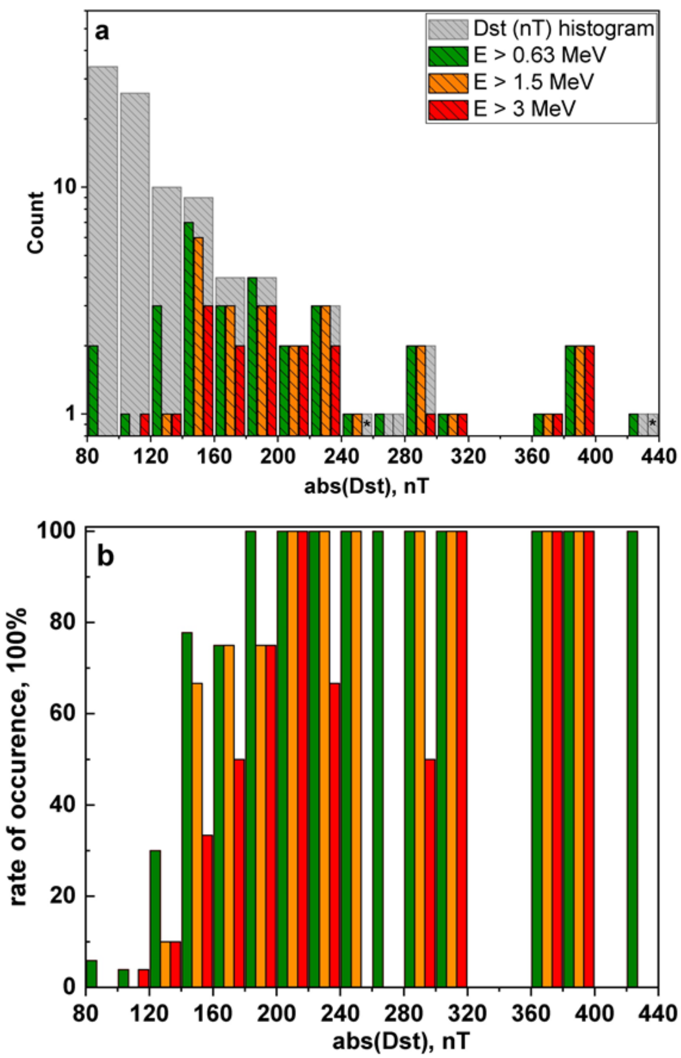

Figure 7. Number of occurrence of SF events for different values of abs(Dst), bin size 20 nT. a) Grey columns height is the number of magnetic storms with abs(dst) maximum in a given bin. Colour columns correspond to the number of SF events in a given bin, green for E>0.63 MeV; orange – for E > 1.5 MeV; red – for E>3 MeV. Stars symbols (*) denote special events when the electron flux E > 3 MeV decreased after the space weather event; b) Relative rate of occurrence of SF events in a given bin of abs(Dst).

The second case in Table 2 of a decrease of the flux of electrons with E > 3 MeV happened following the May 15, 2005 magnetic storm, with Dst = -247 nT (event #32, Table 2). This event was also identified in previous studies, for example, in Tverskaya et al. (2007), who described it as "the devastation of the outer belt on May 15, 2005". These two events demonstrate that in some cases, as it was supposed by Reeves et al. (2003), combination of loss and acceleration processes, both enhanced during strong magnetic storm, can lead to decrease of electron flux.

7. SF events and Kp index

One of the most popular global indices of geomagnetic activity is Kp, used not only for the monitoring and forecast of general space weather conditions, but also in evaluation and forecast of the electron belt dynamics, including the slot region (Borovsky and Spritz, 2017; Glauert et al., 2018 and references therein). Representing the magnetic variations in mid- and sub- auroral latitudes (Mayaud, 1980, and Thomsen, 2004), this index should better account for the effects of not only large CME-driven geomagnetic storms, but also for the effects of the high speed solar wind streams, associated with co-rotating interaction region, with their tendency to produce enhancements of the high energy electrons (Lam et al., 2012).

As follows from the list of events in Table 2, almost all SF events are associated with Kp ≥7. Only during event #23, June 18, 2003, Kp index was just below 7 (7-). As the geomagnetic disturbance was relatively weak, this event was noticed only in the lowest energy channel (E > 0.63 MeV).

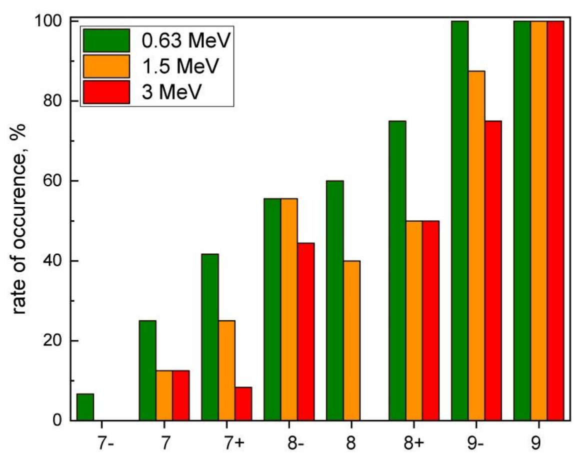

Figure 8. Relative rate of occurrence of SF events for different Kp values, green bars for E>0.63 MeV, orange – for E > 1.5 MeV, and red for E>3 MeV.

Figure 8 provides rate of occurrence of SF events for different values of the Kp index, where Kp is taken as the maximum value per preceding geomagnetic storm. Green, orange and red bars correspond to the occurrences of SF events for electrons in E > 0.63 MeV, E > 1.5 MeV, and E >

3 MeV respectively. For electrons with E > 0.63 MeV the rate of occurrence gradually increases with increasing Kp, achieving 100% at Kp=9-. For higher energy electrons, Figure 8 shows the increase of the rate of occurrence with increase of Kp , achieving 100% for all energies at Kp=9.

8. SF events and hourly range geomagnetic indices

To provide a more detailed description of the geomagnetic variations, data from several geomagnetic observatories were chosen for further analysis. These selected observatories are involved in the definition of Kp index. They are Fredericksburg (FRD), L≈ 2.34, Ottawa (OTT), L ≈ 3.19 and Meanook (MEA), L ≈ 4.56. L-coordinates for these observatories were calculated for epoch 2000 with use of the NASA online tool https://omniweb.gsfc.nasa.gov/vitmo/cgm.html which, in turn, is based on the method of Tsyganenko et al. (1987). Geomagnetic coordinates for Ottawa and Fredericksburg observatories are close to the L-coordinates defined for the slot.

The 1-min geomagnetic data from the observatories were used to calculate an hourly range index (i.e. difference between maximum and minimum values in one hour, maximum between two horizontal components). This index is not influenced by quiet day variations and provides an index that better represents the space-weather related variability of geomagnetic field at the relevant latitudes (L-shells) (Hruska and Coles, 1987).

Similar to Dst and Kp, the occurrence rates of SF events for the whole period 1998-2007, are presented on Figure 9 (a-c) for each of these observatories. Green columns provide the occurrence of SF events for electrons with E > 0.63 MeV, orange ones are for electrons with E > 1.5 MeV, and red ones for electrons with E > 3 MeV, bin size is 100 nT in HR_OBS (i.e. for any observatory).

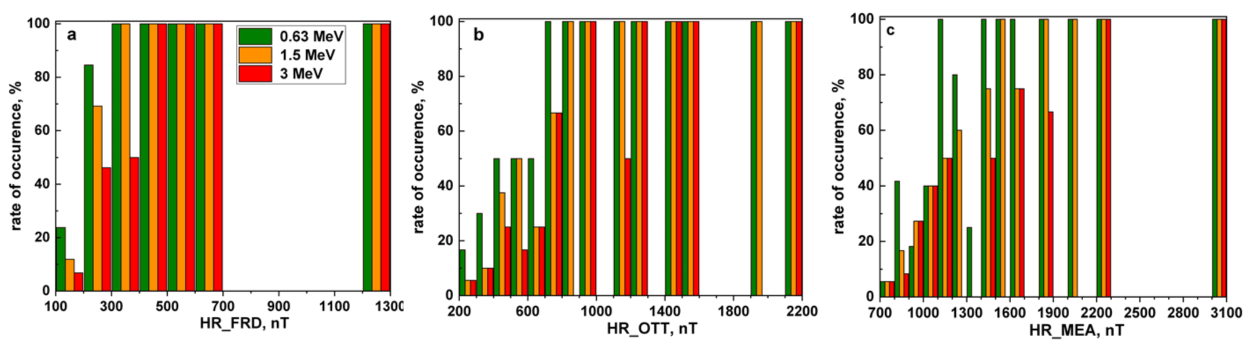

Figure 9. Rate of occurrence of SF events depending on geomagnetic activity at Fredericksburg (a), Ottawa (b) and Meanook (c), bin size 100nT; E>0.63 MeV (green); E > 1.5 MeV (orange); E>3 MeV (red).

Rate of occurrence for SF events is plotted on Figure 9, a) for FRD, b) for OTT, and c) for MEA. At first, it has been found that the thresholds for SF events are associated with the hourly range indices exceeding 100 nT in FRD, 200 nT in OTT, and 700 nT in MEA.

The rate of occurrence increases with increasing of magnetic activity for all the observatories. Best correspondence between geomagnetic activity and SF events is povided by hourly range index based on data from FRD observatory (Figure 9a). Thus, all the geomagentic storms when HR_FRD exceeded 300 nT were followed by SF events in E >0.63 MeV and E > 1.5 MeV, and starting with the geomagnetic hourly range 400 nT, i.e. for HR_FRD > 400 nT, SF events were identified in all three energy channels with 100% rate of occurrence. In regards to hourly range index based on Ottawa geomagnetic data (Figure 9b), it can be concluded that HR_OTT > 700 nT provides 100% rate of occurrence of SF events in E > 0.63 MeV, and E>1.5 MeV, and HR_OTT > 1200 nT provides 100% rate of occurrence of SF events in all three energy channels.

Correspondance of the geomagnetic activity in Meanook to the SF events (Figure 9c) does not show same general trend, as with FRD and OTT. The expected is the increase in rate of occurrence at higher energy channels with the increase of the geomagnetic activity, while for MEA it does not always the case. 100% rate of occurrence in all three energy channels is achieved only for high values of geomagnetic variations, when HR_MEA exceeded 2000 nT.

9. Maximum electron flux in the slot during SF event with relation to geomagnetic activity

In this section, the maximum value of the electron flux per SF event is compared with the corresponding geomagnetic activity to find a relationship between these two parameters. For this, the geomagnetic activity was represented in two ways: first, by the maximum value of the geomagnetic indices per magnetic storm, such as maximum value of (*abs(Dst))* and maximum value of (*HR_OBS*), and second, by the average geomagnetic activity, calculated with use of the geomagnetic variations during two days of the magnetic storm <*abs(Dst)*> and <*HR_OBS*>.

The regression analysis was performed for events identified in Table 2 between the maximum of the electron flux per SF event and the preceding geomagnetic activity(with exception of events #20 and #30 in E>0.63 MeV due to data gaps). A power law relationships have been assumed for the electron flux in E >0.63 MeV and E > 1.5 MeV and an exponential relationship has been assumed for E > 3 MeV. Comparison of the correlation coefficients (see Table 3) demonstrates that use of 2 days average geomagnetic activity preceding SF event provides a more statistically significant regression model than the use of a maximum of the geomagnetic variations.

Table 3.

Correlation coefficients for the regression between the maximum electron flux per SF event and corresponding geomagnetic activity.

Energy band	Correlation with Dst		Correlation with HR_MEA		Correlation with HR_FRD		Correlation with HR_OTT	
	Max	2 days average	Max	2 days average	Max	2 days average	Max	2 days average
E > 0.63 MeV	0.57	0.60	0.42	0.63	0.65	0.74	0.71	0.81
E > 1.5 MeV	0.63	0.66	0.26	0.54	0.67	0.83	0.58	0.83
E > 3 MeV	0.65	0.69	0.26	0.66	0.5	0.74	0.63	0.89

Examples of regression models derived with use of two days average of abs(Dst), HR_OTT and HR_FRD are plotted on Figure 10 where red circles correspond to SF events and the dash blue line represents the regression line. The regression coefficients for these models with use of two days average <HR_FRD>, <HR_OTT>, <HR_MEA> and <abs(Dst)> are provided in Table 4.

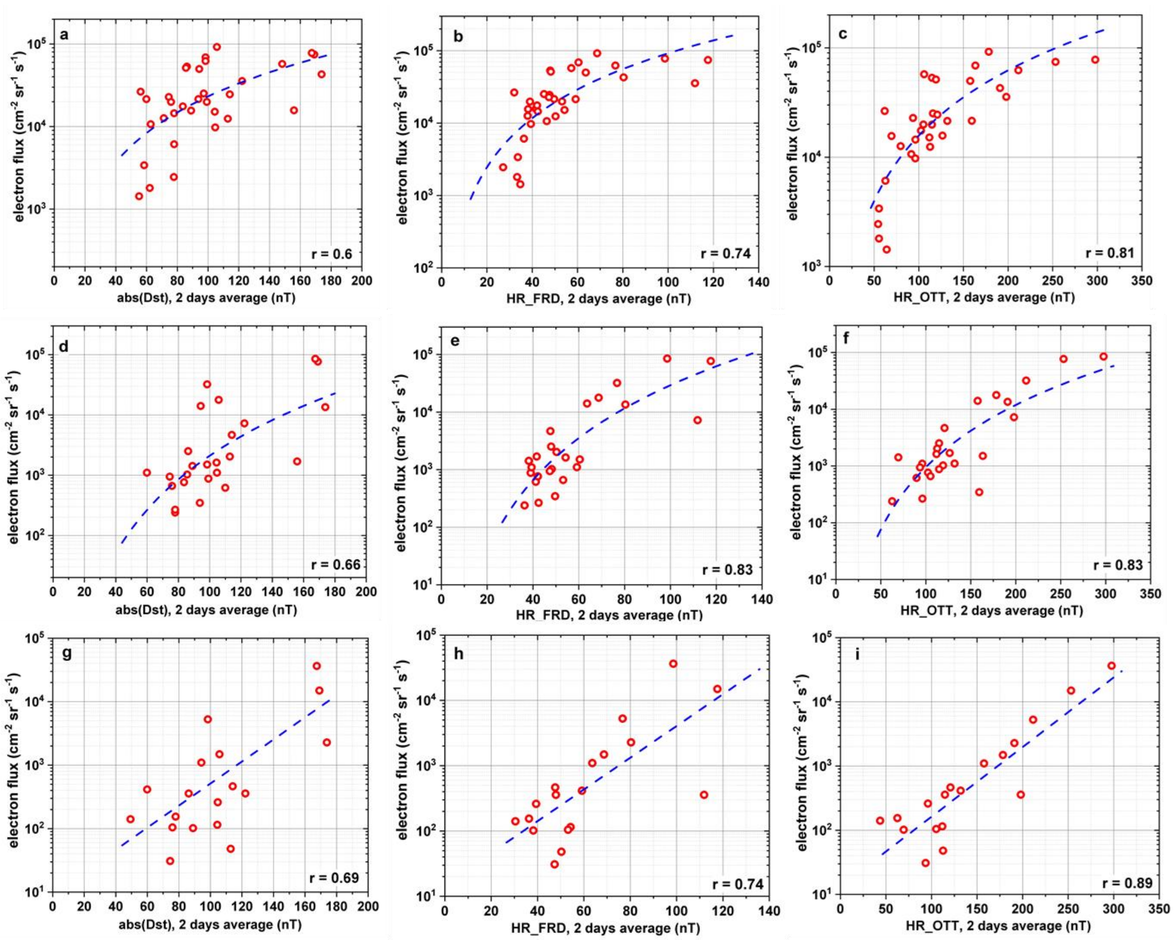

Figure 10. Regression curves (blue dash lines) between the maximum electron flux for each SF event (red circles) and average geomagnetic activity: with <abs(Dst)> (a,d,g); with <HR_FRD> b,e,h); with <HR_OTT> (c,f,g). Top panels (a,b,c) for E > 0.63 MeV, middle panels (d,e,f,) for E > 1.5 MeV, bottom panels (g,h,i) for E > 3 MeV.

Table 4.

Regression coefficients for relationship between the maximum electron flux in the slot and 2 day average of geomagnetic indices.

Energy band	E > 0.63 MeV			E > 1.5 MeV			E > 3 MeV		
Model	$ln(F) \sim a + b * ln(< HR\_OBS >)$						$ln(F) \sim a + b *< HR\_OBS >$		
	corr	a	b	corr	a	b	corr	a	b
HR_FRD	0.74	1.1	2.3	0.83	-8.8	4.1	0.74	2.7	0.056
HR_OTT	0.81	0.6	2.0	0.83	-9.9	3.6	0.89	2.6	0.025
HR_MEA	0.63	-1.5	2.0	0.54	-9.9	3.1	0.66	2.2	0.013
Model	$ln(F) \sim a + b * ln(< abs(Dst) >)$						$ln(F) \sim a + b *< abs(Dst) >$		
	corr	a	b	corr	a	b	corr	a	b
Dst	0.60	0.84	2.0	0.66	-11.0	4.1	0.69	2.24	0.038

As follows from Table 4, in terms of the local hourly range indices, the correlation coefficients are better with the indices obtained from stations with approximate locations corresponding to the L-coordinates of the slot. Fredericksburg observatory has a proper location, with L coordinate inside the slot region, and the electron flux demonstrates good correlation 0.74-0.83 with hourly range index obtained with the data from this observatory. Position of Ottawa observatory at the inner edge of the outer belt makes it good for the description of the dynamics of this inner part of outer radiation belt during the SF events. As a result, the electron flux in the slot region demonstrates good correlation with index, based on data from Ottawa observatory, ranging 0.81-0.89. The correlation with Meanook data and with Dst index is less, in the range 0.54-0.66 for HR_MEA and 0.60-0.69 for Dst. Meanook is at a higher latitude, so is on larger L-shell and, therefore, is less related to the slot region content. At the same time, the Dst index is associated with ring current intensification and is less sensitive to the auroral electrojets, while the strong geomagnetic storms are a combination of these two current systems.

It can be concluded that the geomagnetic activity indices based on the data from two observatories, Ottawa and Fredericksburg, can be used in the assessment of the maximum electron flux in the slot region during SF event.

10. Cumulative time of enhanced geomagnetic activity and long-term variation of the electron flux in the slot region.

The dynamics of electron flux in the slot region is defined by two time-scales. Short-term, lasting several days, penetration of electrons into the slot region and the subsequent long-term attenuation of the electron flux which can be interrupted by the next magnetic storm. As a result, long-term average value of electron flux in the slot region and its variation is impacted not only by intensity of each single magnetic storm, but as well by the total number of strong magnetic storms during a certain period of time.

To illustrate the impact from cumulative time of enhanced geomagnetic activity on the electron flux, Figure 11 presents the monthly average electron flux in the slot region during years 1998-2007 together with the monthly cumulative time when geomagnetic activity exceeded a certain threshold.

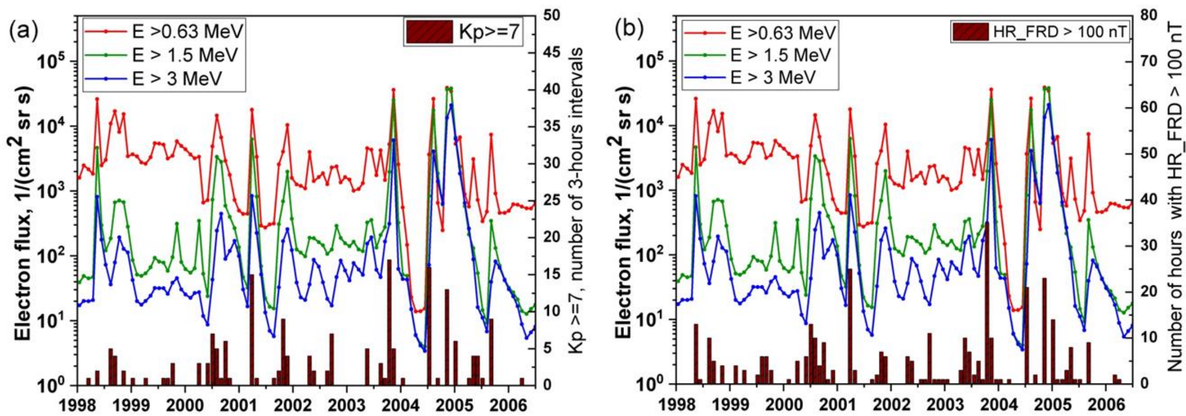

Figure 11. Monthly average electron flux with a) the number of 3-hour intervals when Kp ≥ 7 during one month, b) with the number of hours when HR_FRD > 100 nT during one month.

Red, green and blue curves provide the monthly average electron flux for E > 0.63 MeV, E > 1.5 MeV and E > 3 MeV respectively.

Brown bars represent the cumulative time of enhanced geomagnetic activity. On Figure 11a brown bars correspond to the cumulative time during one month when Kp was ≥ 7 (total number of 3-hour intervals) and on Figure 11b brown bars represent the cumulative number of hours during one month when HR_FRD exceeded 100 nT. These thresholds for SF events with respect to Kp and HR_FRD are the same as determined in Sections 7 and 8. On both plots (Figure 11 a,b) a sharp increase of geomagnetic activity is often closely followed by a sharp increase of the electron flux, with subsequent attenuation of the flux seen over several months after the event, until the next increase of geomagnetic activity.

Decay time of the electron flux in the slot region depends on the energy band and can vary from tens to hundreds of days. Thus, as estimated in *Ripoll et al., 2015*, based on HEO-3 data, the mean life time for electrons at L=2.5 is about 1 month for the 0.63 MeV energy band, about 3 months for 1.5 MeV electrons, and close to 6 months for 3 MeV electrons.

Combined effect of these two processes, the relatively quick increase of the electron flux after space weather events and long decay result in the substantial similarity of the large periods (several months) variation of the electron flux with the cumulative time of enhanced geomagnetic activity. This is illustrated by Figure 12, which shows variations of the six months average electron flux in the slot region together with the cumulative time of enhanced geomagnetic activity. Cumulative time of enhanced geomagnetic activity is represented by browns bars, which are, similar to Figure 11, the total for six months number of intervals when Kp index was ≥ 7 (Figure 12 a) and the total for six months number of hours when *HR_FRD* exceeded 100 nT (Figure 12b).

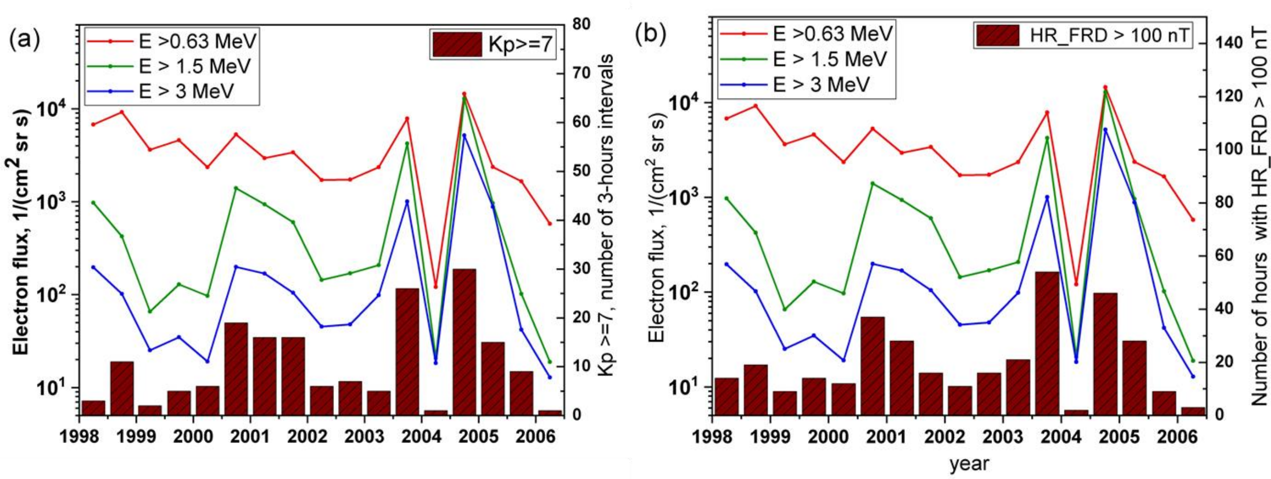

Figure 12. 6 month average of the electron flux with the number of 3-hour intervals when Kp>=7 (a), and with the number of hours when HR_FRD over 100 nT (b).

Correlation between the cumulative time of enhanced geomagnetic activity and six month average of the electron flux in the slot region is shown in Table 5, for all the considered geomagnetic indices. The cumulative time of enhanced geomagnetic activity was defined as a number of intervals (3-hour intervals for Kp and hourly intervals for Dst and HR_OBS) above a threshold. The thresholds for each geomagnetic index correspond to the thresholds for SF events determined in Sections 6-9, namely Kp ≥ 7, HR_FRD > 100 nT, HR_OTT > 200 nT, HR_MEA > 700 nT, and abs(Dst) > 95 nT.

Table 5.

Correlation between six months average of the electron flux in the slot and the cumulative duration of enhanced geomagnetic activity (above a threshold)

	Threshold	E > 0.63 MeV	E > 1.5 MeV	E > 3 MeV
Kp	>=7	0.63	0.89	0.87
HR_FRD	>100 nT	0.67	0.89	0.87
HR_OTT	>200 nT	0.72	0.87	0.83
HR_MEA	> 700 nT	0.61	0.79	0.79
Abs(Dst)	> 95 nT	0.62	0.72	0.6

From Table 5 it can be concluded that correlation between long-term variations of the electron flux in the slot and geomagnetic activity is greater than 0.6 in all magnetic indices. The correlation coefficients for E >1.5 MeV and E> 3 MeV are higher than for E > 0.63 MeV indices, due to the time scale of attenuation of the electron flux in this energies which is close to the averaging period of six months.

The best correlation is demonstrated with the Kp index and magnetic data from Ottawa and Fredericksburg observatories. These results are in agreement with the conclusions obtained in previous sections where it was shown that data from geomagnetic observatories with L-coordinates close to the slot region provides better agreement with the electron flux in the slot. Here Kp index was added to regression analysis and demonstrates as well good agreements with electron flux in the slot, as it is mostly based on data from observatories with L-coordinates close to the L-range of the slot region.

11. Summary

Radiation environment in the slot region between the two electron belts was studied using data from the HEO-3 mission in 1998-2007. Analysis of the slot filling events and the associated geomagnetic disturbances was made for the electron flux in three energy channels, E > 0.63 MeV, E > 1.5 MeV, and E > 3 MeV.

Slot filling events were defined as those times when the slot region was filled by energetic electrons after geomagnetic storms with the flux increasing to values at least twice comparing to those of pre-storm conditions. During 1998-2007 years, 35 space weather events were followed by enhancement of the electron flux in the slot region, in at least one energy channel. Among them, 34 SF events were identified in E > 0.63 MeV, 25 events in E> 1.5 MeV, and 19 in E > 3 MeV. Only 18 of these events were recorded simultaneously in all three energy channels (see Table 2).

Several geomagnetic indices have been used in this study to analyse the relationship between geomagnetic activity and the electron flux in the slot region. These indices include Dst, Kp and local indices of geomagnetic activity which are defined by the hourly range of the geomagnetic variations at three geomagnetic observatories, Fredericksburg, Ottawa and Meanook.

The thresholds for slot filling events were determined in all these geomagnetic indices. Thus, it was defined that all slot filling events were associated with the geomagnetic variations which exceeds 95 nT in abs(Dst), 100 nT in hourly range for FRD, 200 nT in Ottawa hourly range, and 700 nT in MEA hourly range. For Kp index this threshold was Kp ≥7 for almost all the SF events except one event with Kp=7-, which was observed only in E>0.63 MeV.

Rate of occurrence of slot filling events was assessed in relation to different levels of geomagnetic activity. A regression analysis was then done to determine a correlation between the maximum electron flux in the slot region after space weather events and preceding geomagnetic activity. It was shown that not only the intensity of a space weather event but also the cumulative time of enhanced geomagnetic activity has a large impact on dynamics of the electron content in the slot region.

The study has shown that good correlation with the electron content in the slot is provided by geomagnetic data measured close to L-shells of the slot region. Thus, it was shown that the hourly range of geomagnetic activity from Ottawa and Fredericksburg observatories are in a good agreement with the occurrence of slot filling events and intensity of the electron flux in the slot region after a space weather event. For estimation of long-term (several months) variation of the electron flux in the slot region it was recommended to use a cumulative time of exceedance of a geomagnetic activity threshold as demonstrated with magnetic data from Ottawa and Fredericksburg observatories as well as with the Kp index.

12. Conclusion

This study has shown that the electron content of the slot region is well correlated with frequency and intensity of geomagnetic storms, especially with the geomagnetic activity recorded close to projection of the slot region to the Earth surface. Based on the analysis of all the slot filling events and dynamics of the electron flux during the period 1998-2007, covering almost a complete solar cycle, indices of geomagnetic activity with the best correlation with the electron flux in the slot region were determined. Models have been established that use geomagnetic indices to assess the maximum value of the electron flux in the slot region directly after space weather events and the long-term variation of the electron flux in the slot region. The results obtained can be used for hazard assessment of dynamics of the radiation environment in the slot region during periods of different levels of geomagnetic activity and for estimation of the total radiation deposited on a spacecraft passing through the slot region.

13. Acknowledgements

We acknowledge the staff of AeroSpace Corporation for making available data from HEO-3 mission and personally T.P. O'Brien and J.F. Fennel for useful discussions; we would like to acknowledge the staff of the Geomagnetic Laboratory, Natural Resources Canada for providing the geomagnetic data. We would like to thank B.T.Tsurutani for his insightful comments. We express our appreciation for the work of the Prof. L.V. Tverskaya whose outstanding dedication and work on radiation belts dynamics has inspired us to do this research.

Availablilty of data and on-line resources: HEO-3 data are available on http://vibro.org/HEO; Dst and Kp indices were obtained from the World Data Center for Geomagnetism, Kyoto, http://wdc.kugi.kyoto-u.ac.jp/; data from geomagnetic observatories are available from Intermagnet (Ohttps://www.intermagnet.org/). On-line tool for calculation of L-coordinate is available on https://omniweb.gsfc.nasa.gov/vitmo/cgm.html

References

Baker, D.N.S., Blake, J.B., Callis, L.B., Cummings, J.R., Hovestadt, D., Kanekal, S., Klecjer, B., Mewaldt, R.A. & Zwickl, R.D. (1994). Relativistic electron acceleration and decay time scales in the inner and outer radiation belts: SAMPEX. *Geophysical Research Letters, 21*(6), 409-412. https://doi.org/10.1029/93GL03532 .

Baker, D.N., Erickson, P.J., Fennell, J. F., Foster, J. C., Jaynes, A. N., & Verronen, P.T. (2018). Space Weather Effects in the Earth's Radiation Belts, *Space Science Reviews, 214*(1), article id 17, 60 pp.

Baker, D. N., Kanekal, S.G., Li,X., Monk, S.P., Goldstein, J., & Burch, J.L. (2004). An extreme distortion of the Van Allen belt arising from the Halloween solar storm in 2003. *Nature, 432*, 878–881, doi:10.1038/nature03116

Borovsky, J. E., & Shprits, Y. Y. (2017). Is the Dst index sufficient to define all geospace storms? *Journal of Geophysical Research: Space Physics, 122*, 11,543–11,547. https://doi.org/101002/2017JA024679

Falkowski, B. J., Tsurutani, B.T., Lakhina, G.S., and Pickett, J.S. (2017). Two sources of dayside intense, quasi-coherent plasmaspheric hiss: A new mechanism for the slot region? *Journal of Geophysical Research: Space Physics, 122*, 1643–1657. doi:10.1002/2016JA023289.

Glauert, S. A., Horne, R. B., & Meredith, N. P. (2018). A 30-year simulation of the outer electron radiation belt. *Space Weather, 16*, 1498– 1522. doi.org/10.1029/2018SW001981

Hruska, J., & Coles R.L. (1987). A new type of magnetic activity forecast for high geomagnetic latitudes. *Journal of Geomagnetism and Geoelectricity, 39*, 521-534.

Kavanagh, A.J., Cobbett, N., & Kirsch, P. (2018). Radiation belt slot region filling events: Sustained energetic precipitation into the mesosphere. *Journal of Geophysical Research: Space Physics, 123*, 7999-8020. doi.org/10.1029/2018A025890

Lam, H.-L., Boteler, D.H., Burlton, B., & Evans, J. (2012). Anik-E1 and E2 satellite failures of January 1994 revisited. *Space Weather, 10*, S10003. doi:10.1029/2012SW000811

Lazutin, L.L., & Kozelova, T.V. (2011). Energetic electron injections to the inner magnetosphere during magnetic storms and magnetospheric substorms. *Physics of Auroral Phenomena*

(Proceedings XXXIV Annual Seminar, 17-20). Apatity, Russia. Retrieved from http://pgia.ru:81/seminar/archive/2011/1_storm/01_storm_L.L.%20Lazutin,%20T.V.%20Kozelova.pdf

Lyons, L.R., & Thorne, R.M. (1973). Equillibrium structure of radiation belt electrons. *Journal of Geophysical Research*, *78*(13), 2142-2149. doi.org/10.1029/JA078i013p02142

Mayaud, P.N. (1980). Derivation, meaning and use of geomagnetic indices. *Geophysical Monograph Series*, (Vol.22), 154 pp. Washington, D. C.: American Geophysical Union. doi:1029/GM022.

Meredith, N.P., Horne, R.B., Glauert, S.A., & Anderson, R.R. (2007). Slot region electron loss timescale due to plasmaspheric hiss and lightning-generated whistlers. *Journal of Geophysical Research*, *112*, A08214. doi:10.1029/2007JA012413

Nagai, T., Yukimatu, A.S., Matsuoka, A., Asai, K.T., Green, J.C., Onsager, T.G., & Singer, H.J. (2006). Timescales of relativistic electron enhancements in the slot region. *Journal of Geophysical Research*, *111*, A11205. doi:10.1029/2006JA011837

Onsager, T. G., Rostoker, G., Kim, H.-J., Reeves, G.D., Obara, T., Singer, H.J., & Smithtro, C. (2002). Radiation belt electron flux dropouts: local time, radial and particle-energy dependence. *Journal of Geophysical Research*,*107*(A11), 1382. doi:10.1029/2001JA000187

Reeves, G. D., Friedel, R.H.W., Larsen, B.A., Skoug, R.M., Funsten, H.O., Claudepierre, S.G., Fennell, J.F., Turner, D.L., Denton, M.H., Spence, H.E., Blake, J.B., & Baker, D.N. (2016). Energy-dependent dynamics of keV to MeV electrons in the inner zone, outer zone, and slot regions. *Journal of Geophysical Research. Space Physics*, *121*, 397-412. doi:10.1002/2015JA021569

Reeves, G.D., McAdams, K.L., Friedel, R.H.W., & O'Brien, T.P. (2003). Acceleration and loss of relativistic electrons during geomagnetic storms. *Geophysical Research Letters*, *30*(10), 1529-1532. doi:10.1029/2002GL016513

Ripoll, J.-F., Chen, Y., Fennell, J.F., & Friedel, R.H.W. (2015). On long decays of electrons in the vicinity of the slot region observed by HEO3. *Journal Geophysical Research. Space Physics*,*120*, 460–478. doi:10.1002/2014JA020449

Roederer, J.G. (1970). *Dynamics of Geomagnetically Trapped Radiation*. New York: Springer. doi.org/10.1007/978-3-642-40300-3

Roedered, J.G., & Lejosne, S. (2018). Coordinates for representing radiation belt particle flux. *Journal of Geophysical Research: Space Physics, 123*, 1381-1387. doi.org/10.1002/2017JA025053

Sandberg, I., Daglis, I.A., Heynderickx, D., Truscitt, P., Hands, A., Evans, H., & P.Nieminen (2014). Development and validation of the electron slot region radiation environment model. *IEEE Transactions of Nuclear Science, 61*(4), 1656-1662. doi:10.1109/TNS.2014.2304982

Sicard-Piet, A., Boscher, D., Lazaro, D., Bourdarie, S., & Rolland, G. (2014). A new ONERA-CNES slot electron model. *IEEE Transactions on Nuclear Science, 61*, 1648-1655. doi:10.1109/TNS.2013.2293346

Thomsen, M. F. (2004). Why Kp is such a good measure of magnetospheric convection. *Space Weather, 2*, S11004, doi:10.1029/2004SW000089.

Thorne, R.M., Shpritz, Y.Y., Meredith, N.P., Horne, R.B., Li, W., & Lyons, L.R. (2007). Refilling of the slot region between the inner and outer electron radiation belts during geomagnetic storms. *Journal of Geophysical Research, 112*, A06203, 11pp. doi:10.1029/2006JA012176

Tsurutani, B. T., Park, S. A., Falkowski, B. J., Lakhina, G. S., Pickett, J. S., Bortnik, J., Hospodarsky, G., Santolik, O., Parrot, M., Henri, P., & Hajra, R. (2018). Plasmaspheric hiss: Coherent and intense. *Journal of Geophysical Research: Space Physics, 123*, 10,009–10,029. doi.org/10.1029/2018JA025975

Tsyganenko, N. A., Usmanov, A.V., Papitashvili, V.O., Papitashvili, N.E., & Popov, V.A. (1987). *Software for computations of the geomagnetic field and related coordinate systems.* Moscow: Soviet Geophysical Committee, 58 pp.

Turner, D.L., Claudepierre, S.G., Fennell, J.F., O'Brien, T.P., Blake, J.B., Lemon, C., Gkioulidou, M., Takahashi, K., Reeves, G.D., Thaller, S., Breneman, A., Wygant, J.R., Li, W., Runov, A., & Angelopoulos, V. (2015). Energetic electron injections deep into the inner magnetosphere associated with substorm activity. *Geophysical Research Letter, 42*(7), 2079–2087. doi:10.1002/2015GL063225

Tverskaya, L.V. (2011). Diagnostic of the magnetosphere based on the outer belt relativistic electrons and penetration of solar protons: review. *Geomagnetism and aeronomy*, *51*(1), 6-22.

Tverskaya, L.V., Ginzburg, E.A., Ivanova, T.A., Pavlov, N.N., P.M. Svidsky, P.M. (2007). Peculiarities of the Outer Radiation Belt Dynamics during the Strong Magnetic Storm of May 15, 2005. *Geomagnetism and Aeronomy*, *47*(6), 696–703.

Zhao, H., Li, X., Baker, D.N., Claudepierre, S.G., Fennell, J.F., Blake, J.B., Larsen, B.A., Skoug, R.M., Funsten, H.O., Friedel, R.H.W., Reeves, G.D., Spence, H.E., Mitchell, D.G., & Lanzerotti, L.J. (2016). Ring current electron dynamics during geomagnetic storms based on the Van Allen Probes measurements. *Journal of Geophysical Research*, *121*(4), 3333–3346. doi:10.1002/2016JA022358

Zhao, H., & Li., X., (2013a). Inward shift of outer radiation belt electrons as a function of Dst index and the influence of the solar wind on electron injections into the slot region. *Journal of Geophysical Research: Space Physics*, *118*, 756-764. doi:10.1029/2012JA018179

Zhao, H., & Li., X., (2013b). Modeling energetic electron penetrating into slot region and inner radiation belt. *Journal of Geophysical Research: Space Physics, 118,* 6936-6945. doi:10.1002/2013JA019240

Zheng, Y., Lui, A.T.Y., Li, X., & Fok, M.-C. (2006). Characteristics of 2-6 MeV electrons in the slot region and inner radiation belt. *Journal of Geophysical Research: Space Physics, 111*, A10204, 11pp. https://doi:10.1029/2006JA011748